

# GeoSDF: Plane Geometry Diagram Synthesis via Signed Distance Field

CHENGRUI ZHANG\*, Xi'an Jiaotong-Liverpool University, China

MAIZHEN NING\*, Xi'an Jiaotong-Liverpool University, China

ZIHAO ZHOU, Xi'an Jiaotong-Liverpool University, China

JIE SUN, Xi'an Jiaotong-Liverpool University, China

KAIZHU HUANG, Duke Kunshan University, China

QIUFENG WANG<sup>†</sup>, Xi'an Jiaotong-Liverpool University, China

Plane Geometry Diagram Synthesis has been a crucial task in computer graphics, with applications ranging from educational tools to AI-driven mathematical reasoning. Traditionally, we rely on computer tools (e.g., Matplotlib and GeoGebra) to manually generate precise diagrams, but it usually requires huge, complicated calculations cost. Recently, researchers start to work on learning-based methods (e.g., Stable Diffusion and GPT4) to automatically generate diagrams, saving operational cost but usually suffering from limited realism and insufficient accuracy. In this paper, we propose a novel framework GeoSDF to automatically generate diagrams efficiently and accurately with Signed Distance Field (SDF). Specifically, we first represent geometric elements (e.g., points, lines, circles) in the SDF, then construct a series of constraint functions to represent geometric relationship, next we optimize such constraint functions to get an optimized field of both elements and constrains, finally by rendering the optimized field we can obtain the synthesized diagram. In our GeoSDF, we define a symbolic language to easily represent geometric elements and those constraints, and our synthesized geometry diagrams can be self-verified in the SDF, ensuring both mathematical accuracy and visual plausibility. In experiments, our GeoSDF synthesized both normal high-school level and IMO-level geometry diagrams. Through both qualitative and quantitative analysis, we can see that synthesized diagrams are realistic and accurate, and our synthesizing process is simple and efficient. Furthermore, we obtain a very high accuracy of solving geometry problems (over 95% while the current SOTA accuracy is around 75%) by leveraging our self-verification property. All of these demonstrate the advantage of GeoSDF, paving the way for more sophisticated, accurate, and flexible generation of geometric diagrams for a wide array of applications. Based on the GeoSDF, we have developed a tool for plan geometry diagram synthesis and will provide the link after the paper review.

CCS Concepts: • **Theory of computation** → **Computational geometry**; • **Computing methodologies** → **Representation of mathematical objects**; *Optimization algorithms*.

\*Both authors contributed equally to the paper

<sup>†</sup>Corresponding author.

Authors' addresses: Chengrui Zhang, Xi'an Jiaotong-Liverpool University, Suzhou, China, chengrui.zhang18@student.xjtlu.edu.cn; Maizhen Ning, Xi'an Jiaotong-Liverpool University, Suzhou, China, maizhen.ning16@student.xjtlu.edu.cn; Zihao Zhou, Xi'an Jiaotong-Liverpool University, Suzhou, China, zihao.zhou22@student.xjtlu.edu.cn; Jie Sun, Xi'an Jiaotong-Liverpool University, Suzhou, China, Jie.Sun@xjtlu.edu.cn; Kaizhu Huang, Duke Kunshan University, Kunshan, China, kaizhu.huang@dukekunshan.edu.cn; Qiufeng Wang, Xi'an Jiaotong-Liverpool University, Suzhou, China, Qiufeng.Wang@xjtlu.edu.cn.

Permission to make digital or hard copies of all or part of this work for personal or classroom use is granted without fee provided that copies are not made or distributed for profit or commercial advantage and that copies bear this notice and the full citation on the first page. Copyrights for components of this work owned by others than ACM must be honored. Abstracting with credit is permitted. To copy otherwise, or republish, to post on servers or to redistribute to lists, requires prior specific permission and/or a fee. Request permissions from [permissions@acm.org](mailto:permissions@acm.org).

© 2025 Association for Computing Machinery.

0730-0301/2025/6-ART \$15.00

<https://doi.org/10.1145/nnnnnnn.nnnnnnn>

Additional Key Words and Phrases: Plane Geometry Diagram Synthesis, Plane Geometry Problems, Math Reasoning, Signed Distance Field

## ACM Reference Format:

Chengrui Zhang, Maizhen Ning, Zihao Zhou, Jie Sun, Kaizhu Huang, and Qiufeng Wang. 2025. GeoSDF: Plane Geometry Diagram Synthesis via Signed Distance Field. *ACM Trans. Graph.* 1, 1 (June 2025), 10 pages. <https://doi.org/10.1145/nnnnnnn.nnnnnnn>

## 1 INTRODUCTION

The study of geometry problems is fundamental across numerous disciplines, serving as a cornerstone for advancements in computer graphics, computational geometry, robotics, architectural design, and even theoretical mathematics. The emergence of large language models (LLMs) has introduced new approaches for addressing Plane Geometry Problems (PGPs) [Shi et al. 2024] by understanding both textual problem descriptions and their corresponding geometric diagrams [Cai et al. 2024; Gao et al. 2025; Lu et al. 2024; Xia et al. 2025; Xu et al. 2024a; Zhang et al. 2024b,a]. Despite significant efforts to enhance the reasoning capabilities of LLMs, the performance of models remains limited by the scarcity of high-quality datasets containing annotated plane geometry diagrams [Zhang et al. 2023b]. Improvements in text-based inputs alone, like G-LLaVA [Gao et al. 2025], are insufficient to compensate for the absence of rich, well-structured graphical representations [Ning et al. 2025; Xu et al. 2024b]. As a result, suboptimal performance appears in model-driven solutions [Deng et al. 2024]. Therefore, our work aims to design an approach to synthesize high-quality plane geometry diagrams.

Recent manual system advancements [Hunter 2007; Kazemi et al. 2024; Team 2024] have led to the development of tools specifically designed to enhance the quality of geometric diagrams. However, as illustrated in Figure 1, manual construction using computer tools such as Matplotlib [Hunter 2007] and GeoGebra [Team 2024] typically requires the explicit specification of element positions. This process is often inflexible and laborious with amount of calculation, as it necessitates adapting to high-level geometric relationships or ensuring the satisfaction of intricate constraints. To accelerate diagram generation, rule-based approaches have been proposed, such as the one in [Kazemi et al. 2024], which employs programmatic techniques to automate construction. Nonetheless, as shown in Figure 1, these methods rely heavily on predefined geometric primitives and fixed assembly rules, which pose limitations when generating diagrams with complex or irregular configurations. The remarkable capabilities of generative models like Stable Diffusion [Rombach et al. 2021] and DALL-E 3 [OpenAI 2024] in producing realistic natural images offer an important insight: it raises the question of whether similar approaches can be leveraged to generate geometric

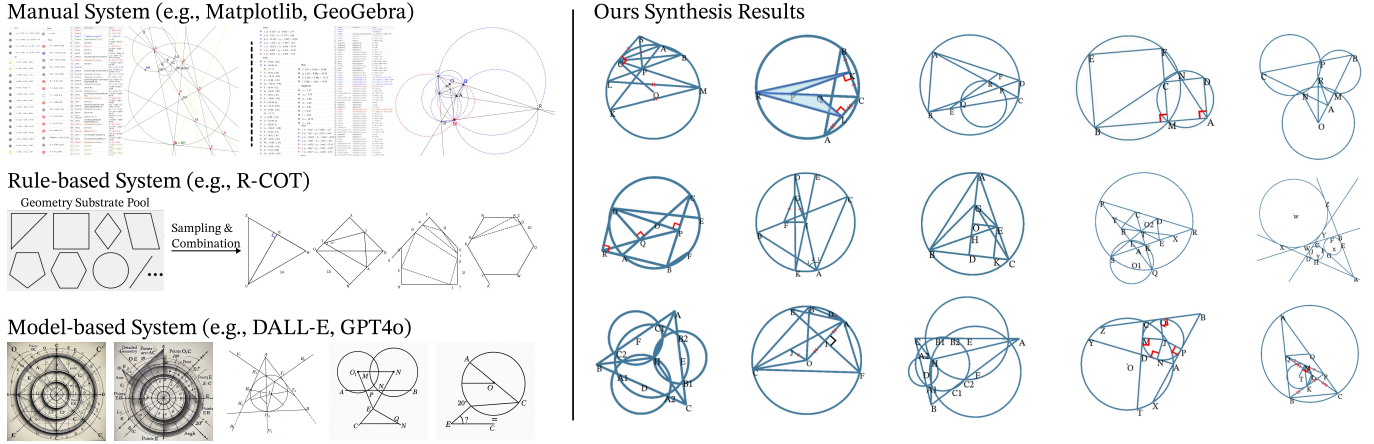


Fig. 1. Comparison of Geometric Diagram Synthesis Methods. This figure illustrates the distinct approaches to generating plane geometric diagrams. Manual systems require tedious coordinate and relation input (left side for each diagram), involving extensive numerical calculations. Rule-based systems (e.g., R-COT [Kazemi et al. 2024]), while structured, struggle with novel, complex, or highly precise mathematical relationships due to their reliance on predefined templates. Model-based systems DALL-E 3 [OpenAI 2024] and GPT4o lack the precision and accurate mathematical synthesis. In contrast, our method synthesizes novel and complex diagrams accurately from elements and constraints without manual calculation. All diagrams are synthesised from the IMO problem set.

diagrams. Unfortunately, as illustrated in Figure 1, these generative models struggle with the deterministic rules and mathematical validity (e.g., exact coordinates, symmetry), resulting in synthesizing inaccurate diagrams [Zhang et al. 2023a,b].

In this paper, we propose a novel framework to automatically synthesize precise **Geometry diagrams** by leveraging **Signed Distance Field (SDF)**, termed as **GeoSDF**. In the theory of SDF, it defines a scalar field that assigns to each point in space a signed distance to the nearest surface of a geometric object [Yariv et al. 2020], thus being differentiable to be optimization. In our proposed GeoSDF, the textual problem description is first parsed into a set of mathematically well-defined components, which we refer to as **elements**. These elements are then governed by a set of **geometric constraints** derived from the problem’s underlying mathematical relationships, such as perpendicularity, parallelism, or incidence. Unlike previous methods, our GeoSDF allows these relationships to be quantitatively expressed—for instance, through the distance from a point to a line—enabling precise and verifiable encoding of geometric structure. These constraints are then incorporated into a loss function, effectively translating the mathematical conditions into an **optimization objective**. By leveraging gradient descent, GeoSDF iteratively refines the positions of elements in the diagram to satisfy complex constraints, allowing for the generation of accurate and mathematically valid geometric figures. This formulation supports both quantifiable relations and the derivation of exact solutions, addressing key limitations of existing diagram generation methods.

In experiments, we synthesize both normal high-school level and IMO-level geometry diagrams, and both qualitative and quantitative analyses demonstrate that the synthesized geometry diagrams are realistic and accurate, verifying the effectiveness. Furthermore, by leveraging the self-verification property, GeoSDF can also be directly applied in solving geometry problems and achieve a very high accuracy, significantly outperforming previous learning based methods,

including advanced LLMs such as GPT and Gemini. For example, we can achieve an accuracy of 95.9% on GeoQA dataset [Chen et al. 2021], which is obviously higher than the current state-of-the-art accuracy (only around 75%). To be noted, our GeoSDF is easy to implement, and the synthesis is efficient. Based on the GeoSDF, we have developed a tool for plan geometry diagram synthesis. The contributions of this paper can be summarized as follows

- We introduce **GeoSDF**, a novel framework that synthesizes plane geometry diagrams accurately. It integrates both structural elements by SDF representation and mathematical constraints within an optimization framework.
- As a key feature of GeoSDF, all geometric relations are inherently quantifiable. The constraint satisfaction and diagram quality can be explicitly evaluated.
- The utilization of quantifiable geometric relations enables our GeoSDF can directly infer accurate solutions to solve geometry problems.
- Extensive experiments demonstrate that diagrams synthesized by GeoSDF are highly accurate and enhance the capabilities of AI models in geometric reasoning.

## 2 RELATED WORKS

### 2.1 Plane Geometry Problem Solving

Early approaches to plane geometry problem (PGP) solving relied on manually defined rules applied to small datasets [Seo et al. 2015, 2014], resulting in poor generalization. Neural network-based models, such as NGS [Chen et al. 2021] and DPE-NGS [Chen et al. 2021], introduced visual question answering and specialized program generation, but still struggle with coarse-grained diagram understanding [Ning et al. 2023]. Symbolic reasoning methods, including InterGPS [Lu et al. 2021] and FormalGeo [Zhang et al. 2023b], use complex rule-based systems to interpret formal languages parsed from diagrams and text. However, their performance is constrained by

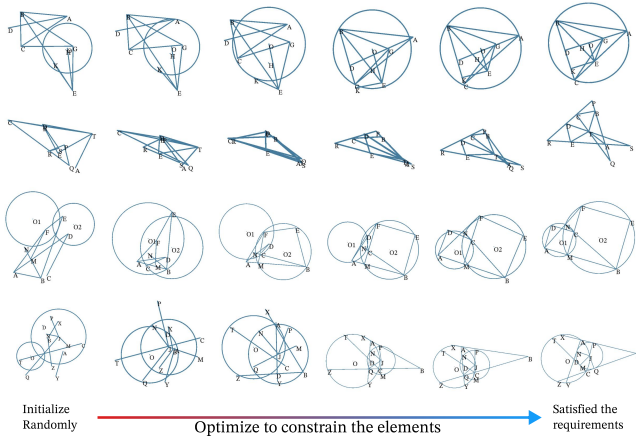


Fig. 2. The visualization of the optimization process. We first randomly initialize the geometry elements and then optimize the SDF by geometry constraints to the synthesized geometry diagram. The upper two examples are selected from FormalGeo-IMO [Zhang et al. 2023b], and the lower two examples are from IMO 1959 Question 5 and IMO 2021 Question 4.

limited datasets and parameter sizes, and they do not produce natural language solutions. Recent advances in multi-modal large language models (MLLMs), such as G-LLaVA [Gao et al. 2025] and Geo-LLaVA [Xu et al. 2024b], fine-tune based models [Liu et al. 2023] to generate natural language solutions. These approaches benefit from data augmentation techniques (e.g., Geo170K via GPT-3.5 [Gao et al. 2025]), but often prioritize textual information over the diversity and complexity of geometry diagrams [Zhuang et al. 2024]. While methods like GeoX [Xia et al. 2025] and R-CoT [Deng et al. 2024] have made progress in diagram understanding, generating accurate, diverse, and controllable geometric diagrams remains a fundamental challenge for advancing GGP solving.

## 2.2 Plane Geometry Diagram Synthesis

Plane geometry diagram synthesis is critical for evaluating problem-solving systems but is underexplored due to complexity [Rom-bach et al. 2022]. Current rule-based methods, including Geom-Verse [Kazemi et al. 2024] and MAVIS [Zhang et al. 2024c], stitch predefined shapes along edges. This limits them, however, from generating diagrams with inscribed relationships (e.g., a triangle in a circle), impacting realism. Despite R-CoT’s [Deng et al. 2024] advancements with inscribed elements, existing approaches remain constrained by predefined shapes and rules, preventing synthesis from textual requirements. Our proposed GeoSDF overcomes this by synthesizing flexible plane geometry diagrams directly from given text constraints.

## 3 METHODOLOGY

In this section, we introduce the method for utilizing geometric elements and constraints to generate diagrams that fulfill all specified constraints. The SDF and geometric terms will be introduced in Sec. 3.1 while Section 3.2 describes our method in details consisting of four steps.

### 3.1 Preliminary

**Signed Distance Field.** A field in mathematics is a function that assigns a value (scalar or vector) to each point in a space. The space provides the coordinate system and the notion of distance necessary. The Signed Distance Field assigns a signed distance to the nearest point on the boundary of the shape for every point in this space. In mathematics, the SDF  $F$  is a scalar field that assigns a value  $s$  to every position  $x$  in the space by

$$F(x) = s, \quad x \in \mathbb{R}^2, s \in \mathbb{R}, \quad (1)$$

The value  $s$  indicates the distance from the position  $x$  to the shape  $\Omega \in \mathbb{R}^2$  in the two-dimensional plane space. The distance between a point  $x$  and the  $\partial\Omega$  boundary of the shape is hereby defined as

$$d(x, \partial\Omega) = \inf_{y \in \partial\Omega} d(x, y),$$

where  $\inf$  denotes the infimum and  $d$  represents the distance. For simplicity, that means the assigned value to the space corresponds to the minimum distance from the point to the geometric shape.

**Elements and Constraints in geometry diagrams.** In geometry, the fundamental elements in 2D Euclidean geometry are Points, Lines, Circles, and Planes. Constraints are conditions or relationships imposed on geometric elements. These constraints restrict the possible configurations or properties of the elements, leading to specific geometric diagrams or relationships. Constraints can be broadly classified into four categories [Berg et al. 2008]: 1) **Incidence Constraints:** These specify that one geometric element lies on another. 2) **Metric Constraints:** These involve measurements such as distances, angles, and areas. 3) **Relative Position and Orientation Constraints:** These define how geometric elements are positioned and oriented with respect to each other. 4) **Topological Constraints:** These describe the connectivity and arrangement of geometric elements, focusing on properties that are preserved under continuous deformations.

### 3.2 Plane Geometry Diagram Synthesis

For synthesizing plane geometry diagrams, our GeoSDF framework mainly consists of four steps as shown in Fig.3.

(1) **Representation of Geometric Elements.** We use the functions to represent basic geometric elements  $E$  in the Signed Distance Field. We define the four types of elements: point, segment, line, and circle. The function defines the distance from each point in space to the shape. By composing the basic elements, we could synthesize the complex shapes in Fig. 3 (b). These functions are parameterized by continuous variables (e.g., coordinates of points, radii of circles, or angles between lines) to control the attributes. In the initial state, we construct the parameters randomly. We sample the SDF by pixel grid directly at the initial state, as shown the Fig. 3 (c).

(2) **Constraints of the Elements.** Once the basic elements are represented, we impose geometric constraints, which define the relationships between these elements, as optimization targets. We define the constraint functions by using a symbolic language, shown in Tab. 1. These constraints are a set of differentiable functions,  $C = \{c_i(E) = 0\}_{i=1}^m$ , where each  $c_i(E)$  represents a specific constraint with elements set  $E = \{e_1, e_2, \dots, e_N\}$  and  $m$  constraints in total. The goal is to find a configuration of the geometric elements,  $E$ ,

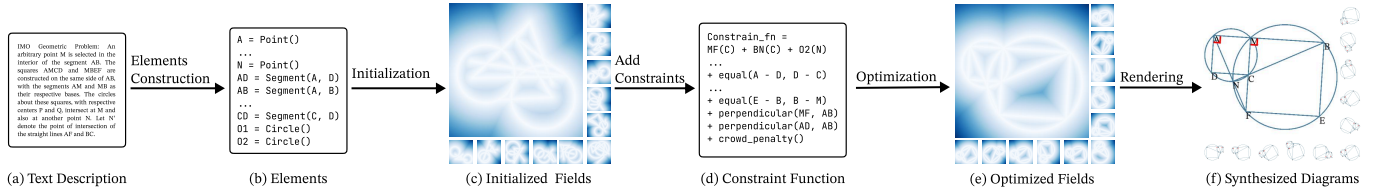


Fig. 3. The GeoSDF Pipeline with an example IMO diagram synthesis process. (a) The description of the figure in natural language. (b) The representation of geometric elements by our symbolic language. (c) The visualization of initialized elements field. (d) Constraints of elements in our SDF. (e) Visualization of the optimized fields. (f) The rendering diagrams. Some parts are omitted due to space limitations.

that satisfies all these constraints. To achieve this, we define a loss function:

$$L(E) = \sum_{i=1}^m c_i(E),$$

where each constraint function  $c_i(E)$  is continuous and differentiable with respect to the parameters of  $E$  shown as Figure 3(d). When the loss reaches its minimum, i.e.,  $c_i(E^*) = 0$  for all  $i$ , where  $E^*$  represents the desired configuration, all constraints are satisfied. It is essential that these constraint functions are differentiable to facilitate gradient-based optimization methods. It is worth noting that through our framework, users can easily define their own loss function according to the required constraints.

(3) **Optimization of the constraints.** Consequently, the geometry synthesizing task becomes a constrained minimization problem to determine the configuration  $E^*$ :

$$\begin{aligned} \min \quad & L(E) \\ \text{subject to} \quad & c_i \geq 0 \text{ for } i = 1 \dots m. \end{aligned}$$

The optimization process converges when the loss reaches a threshold, at which point the configuration  $E^*$  is considered the final geometry diagram, shown as Figure 3(e).

We visualized the process of the optimization of the GeoSDF in Fig. 2 with four IMO examples of the geometry diagrams. The leftmost diagrams represent the initial state, while the rightmost diagrams depict the final state after the optimization process. The initial state is set randomly. Through optimization, the SDF diagrams gradually evolve from a random configuration  $E$  to  $E^*$ , ultimately satisfying the diagram's constraints. The detailed synthesis processes are in the Appendix ??.

During the optimization of the SDF, the loss function may converge to a local minimum, leading to a suboptimal configuration. This can cause the geometry shape  $E^*$  to degrade into a degenerate form, such as a point or a line. In extreme cases, although the geometry may still satisfy most constraints (such as the perpendicularity of two lines), the resulting configuration will appear as a collapsed or overlapping set of elements, like a stack of lines or points, which is visually undesirable. The local minimum can be identified when the shape  $E^*$  degenerates into a point or a line. To overcome this issue, we propose a **crowd regularization term**, which encourages a more spread-out configuration, preventing the elements from collapsing too close together. The regularization term is defined as

$$L_{crowd}(x) = \sum_{1 \leq i < j \leq N} [\max(0, \tau - \|x_i - x_j\|)]^2, \quad (2)$$

where  $\tau$  is the minimum acceptable distance between any pair of elements, and more details are in the Appendix ??.

(4) **Rendering of diagrams.** The explicit representation of the shape's boundary is obtained by sampling the zero iso-surface of the implicit field, as depicted in Fig. 3 (f). This iso-surface is mathematically defined as the boundary of points  $x$  where the signed distance function  $F(x) = 0$ , thereby delineating the underlying planar geometry.

The optimized configuration  $E^*$  allows for sampling the SDF of the geometric elements and evaluating the zero iso-surface to render the corresponding point set. To achieve this, a  $N^2$  pixel grid is sampled. A threshold  $\tau$  is then applied to the SDF values to extract the boundaries of the geometric shapes. This threshold determines the sampling range for the field, and its impact on the visualization is presented in Figure 4. Different threshold values result in varying levels of detail in the geometric diagram; specifically, a higher threshold expands the element boundaries, leading to thicker lines.

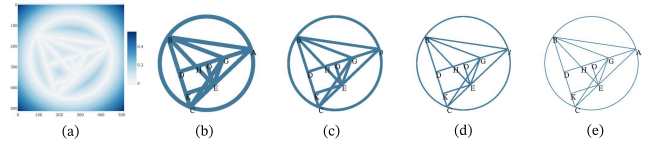


Fig. 4. (a) The values sampled from SDF by  $512 \times 512$  pixel grid visualization. And visualizations of its zero iso-surface with different thresholds (b) 0.03, (c) 0.2, (d) 0.1, (e) 0.005.

## 4 EXPERIMENTS

In this section, we first describe the implementation details, then give results of synthesized diagrams for normal high-school level and IMO level problems in Sec. 4.2 and Sec.4.3, next evaluate the effectiveness of GeoSDF for solving Plane Geometry Problems (PGP) in Sec. 4.4, finally show analysis of our GeoSDF in last three sections.

### 4.1 Implementation Details

During the optimization process, we set the maximum number of iteration steps to 10,000. The learning rate was annealed from an initial value of 0.1 down to  $1 \times 10^{-6}$  using a cosine annealing schedule. We define a successful synthesis when the total constraint loss falls below a threshold of 0.1. We select FormalGeo7k [Zhang et al. 2023b] as the source datasets for providing the base geometry predicates as the input constraints of GeoSDF. FormalGeo7k consists of 6,981

Table 1. Predefined common constraints and loss functions in GeoSDF. In our framework, GeoSDF, we consider these geometric constraints directly as the loss functions to quantify the deviation from the desired configuration. The mathematical details are in Appendix ???. Users could extend the extra loss function easily to satisfy other customized constraints.

Constraint Category	Constraint	Loss Function	Description
Incidence Constraints	Equality	$\text{Equal}(x_1, x_2)$	Two geometric elements $x_1, x_2$ have the same value.
	Less	$\text{Less}(v_1, v_2)$	One numerical value is less than or equal to another.
Metric Constraints	Distance	$\text{Equal}(E(x), v)$	A specific distance $v$ between two geometric elements $E_1(E_2)$ .
	Angle	$\text{Angle}(x_1, x_2, x_3)$	The angle formed by three points $x_1, x_2, x_3$
	Area	$\text{Area}(x_1, \dots, x_n)$	A specific area for a polygon defined by a sequence of points.
	Crowd Penalty	$\text{Crowd}(x_1, \dots, x_n)$	Encourages geometric elements (typically points) to be spaced apart.
Relative Position and Orientation Constraints	Parallelism	$\text{Parallel}(x_1x_2, x_3x_4)$	Two lines or segments are parallel to each other.
	Perpendicularity	$\text{Perpendicular}(x_1x_2, x_3x_4)$	Two line or segments are perpendicular to each other.
	Order	$\text{Order}(x_1, \dots, x_n)$	Counterclockwise order of points $x_1, \dots, x_n$ .
	On	$E(x)$	A specified point $x$ lies on a given segment or circle $E$ .
Topological Constraints	Inside	$\text{Inside}(p, x_1, \dots, x_n)$	A point $p$ if it lies outside a convex polygon defined by other points.
	Convexity	$\text{Convex}(x_1, \dots, x_n)$	A polygon formed by a sequence of points $x_1, \dots, x_n$ is convex.

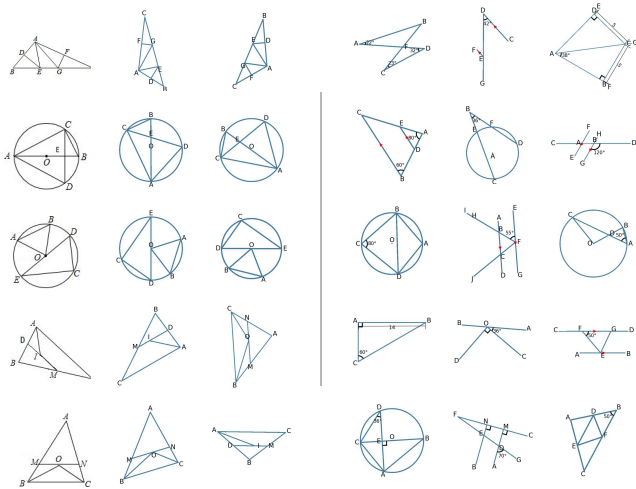


Fig. 5. The visualization of the synthesized geometry diagrams. Left: Synthesis on the FormalGeo7k dataset with diversity, in which the first row is the ground truth. Right: Synthesised with detailed annotations.

PGPs, which were collected and re-annotated from previous PGP datasets, including GeoQA [Chen et al. 2021], GeoQA-Plus [Cao and Xiao 2022], and Geometry3K [Lu et al. 2021]. We leverage the annotated predicates from the FormalGeo7k to synthesize geometry diagrams using GeoSDF by first transforming these predicates into our structural and constraint-based representations and subsequently optimizing the SDF to generate precise and structurally valid geometry diagrams. For the experiments on IMO problems, we use the problems selected by AlphaGeometry [Trinh et al. 2024], and the constraints of these IMO problems were manually annotated by us according to the problem given conditions. In our experiments, we employ an NVIDIA RTX 4090 GPU to accelerate the synthesis of diagrams.

## 4.2 Visualization of Synthesized Diagrams

**Geometry Diagram Synthesis.** We first applied GeoSDF to synthesize geometry diagrams based on the FormalGeo7k dataset. For each problem in the dataset, we leveraged the annotated textual predicates as the problem constraints and then used them to synthesize the corresponding plane geometry diagram. The visualization of five cases of these synthesized diagrams is shown in the left part of Figure 5. For each original problem, we select two new diagrams from the synthesized results, with the top one showing the original diagram (i.e., ground truth) and the other two representing the newly synthesized ones. According to the visualization cases, the synthesized diagrams are visually consistent with the originals but have diverse visual characteristics like rotation, demonstrating GeoSDF’s effectiveness in synthesizing diagrams that have consistent geometric features with original diagrams based on the provided textual predicates. Moreover, the diversity in diagram visual characteristics showcases the GeoSDF’s flexibility and generalization ability, effectively capturing variations while maintaining the underlying geometric relationships. Such flexibility and generalization make GeoSDF a valuable and promising tool for advancing the synthesis and understanding of geometry diagrams in the PGP field.

**Geometry Diagram Synthesis with Annotations.** Furthermore, our method is highly flexible, providing a range of annotations for synthesized diagrams, including parallelism, perpendicularity, lengths, and angles. These annotations are clearly visualized in Figure 5 (right). This capability could not only enhance human readability but also Multi-Modal LLM understanding of geometric diagrams, guiding models to focus on specific geometric relationships rather than relying solely on abstract visual features, especially since visual encoders may not be optimized for these specific tasks.

**Comparison to Existing Methods.** A key limitation of prior methods like GeomVerse [Kazemi et al. 2024] and MAVIS [Zhang et al. 2024c] is their reliance on an initial base geometry (e.g., a closed shape like a rectangle or circle) from which other elements

are progressively added. In contrast, GeoSDF eliminates this requirement, capable of synthesizing an entire diagram from scratch using only points and lines, without any predefined initial shape.

### 4.3 International Mathematical Olympiad Geometry

**4.3.1 IMO Geometry Diagrams Synthesis and Visualization.** A key advantage of GeoSDF is its ability to synthesize complex geometry diagrams, particularly in the context of IMO geometry problems. Previous methods are unable to synthesize these complicated diagrams as they rely on predefined geometric elements and rule-based algorithms to splice these elements together [Deng et al. 2024; Kazemi et al. 2024]. These splicing methods are not capable of synthesizing IMO problems due to the increased complexity and these methods are not capable to synthesize diagrams based on given conditions, the need for more intricate geometric shapes, more complicated relationships between geometric elements, and a greater number of independent lines that are challenging for previous methods to handle. Therefore, we applied GeoSDF to the FormalGeo-IMO dataset, and in Figure 2 of Section 3 we have shown the visualization of the synthesized geometry diagrams for four different IMO problems. These IMO cases are highly complex, each constructed with different geometry elements and relationships. For example, the diagram in the first problem involves intricate inscribed relationships, the second problem is composed of multiple intersecting line segments, and the third and fourth problems require simultaneously handling the relationships between two circles as well as multiple line segments connected to these circles. The synthesized diagrams by GeoSDF are visually and mathematically consistent with the original IMO problems, demonstrating the robust potential of GeoSDF in handling complex geometry tasks.

**4.3.2 Human Evaluation on IMO Geometry Problems.** To evaluate whether the synthesized IMO diagrams preserve the geometric characteristics of the original diagram, we conducted a human evaluation study. We invited 20 participants with bachelor’s degrees in science to assess whether the diagrams generated by GeoSDF are structurally equivalent to the original diagram (i.e., ground truth). A total of 30 IMO geometry problems were used in the evaluation. On average, participants judged that 88.67% (26.6 out of 30) of the synthesized diagrams fully reflected the geometry information in the original problem diagram. This result highlights that GeoSDF exhibits strong capability in synthesizing diagrams for IMO-level problems. The design of the questionnaire is included in Appendix ??.

### 4.4 Quantifiability of GeoSDF

One of the significant property of GeoSDF is the quantifiability. It means that all elements of the geometry diagram can be directly quantified or measured (e.g. degree of angle) and extracted (area and length will be scaled through the scale bar of each case). For example, the first problem in Fig. 6 asks for the measure of angle CDE (marked by the red arrow). Once the SDF optimization is complete and the diagram meets the loss constraint, we extract the angle value as the solution, which is 55. Similarly, in another example from Fig. 6, we determine the length of line YZ, the diameter of circle M. This capability enables us to extend its application to a broader range of

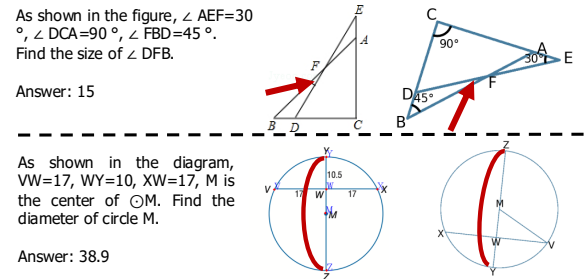


Fig. 6. The example of quantifiability of GeoSDF. Our method is able to measure all the values in the diagram (e.g. degree, area), where the left diagram is the original diagram and the right one is synthesised by GeoSDF.

experiments, such as direct problem solving and verifying whether the synthesized diagrams precisely satisfy the original problem.

**4.4.1 Plane Geometry Problem Solving.** In this way, we conduct the plane geometry problem (PGP) solving task on the GeoQA [Chen et al. 2021] dataset and comparing with various SOTA solvers including general neural-based and MLLM-based methods. Specifically, we first synthesize the SDF representation of the problem by constructing it from the symbolic clauses given by the problem. We then measure the values of the target elements in the problem, treating them as the solution. This approach corresponds to the completion setting, where the solution value is directly output. The experiment results are shown in Table 2. Surprisingly, due to its high accuracy in diagram synthesis, our method achieved a 94.5% accuracy rate under the completion setting, significantly outperforming all current SOTA solvers, including both neural-based and MLLM-based PGP solvers. These results demonstrate the strong potential of our approach for solving PGPs. In the Choice setting, our method also significantly outperforms other models, including multi-modal LLMs equipped with Chain-of-Thought reasoning or specifically fine-tuned for PGP solving tasks. Notably, our method relies solely on the basic problem information parsed from the original input using FormalGeo, without incorporating any additional data which ensuring a fair comparison with other models. These experiments highlight the strong potential of applying GeoSDF in the field of PGP solving research. GeoSDF also shows promise as a practical tool to support the development of PGP solvers, like serving as an external module for solution verification or diagram-based reasoning.

**4.4.2 Synthesised Diagram Structural Equivalence Check.** In addition, when using GeoSDF to synthesize diagrams based on known problem statements, questions, and answers, the quantifiability of GeoSDF enables further verification of whether the synthesized diagrams satisfy the given conditions and correspond to the correct answers. If the values extracted from the SDF representation align with the expected solution and the optimization loss remains below a predefined threshold, we consider the diagram a faithful representation of the original problem. This verification process uses the problem’s goal formula to locate and extract relevant geometric features from the SDF object. To quantify this, we evaluated the success rate of diagram synthesis on the FormalGeo7K dataset. Among 6,981 samples, 5,943 diagrams (85.13%) passed the loss constraint

Table 2. Accuracy (%) on the GeoQA test set and reported for two settings: **Completion**, the answer value is directly outputted; **Choice**, the problem choice is directly outputted. For neural PGP solvers, a random choice is selected if the completion result doesn't match any given choice.

Model	Completion	Choice
NEURAL PGP SOLVERS		
NGS[Chen et al. 2021]	60.0	69.5
DPE-NGS[Cao and Xiao 2022]	62.7	70.4
SCA-GPS[Ning et al. 2023]	64.1	72.7
CLOSED SOURCE MLLMs		
GPT-4o	-	61.4
Gemini-2.5	-	63.4
MLLM PGP SOLVERS		
G-LLaVA-13B[Gao et al. 2025]	-	67.0
GeoX[Xia et al. 2025]	54.9	-
Qwen2.5-VL-7B[Bai et al. 2025]	64.2	64.3
InternVL2.5-8B[Chen et al. 2024]	50.5	58.1
MAVIS-7B[Zhang et al. 2024c]	-	68.3
R-CoT-8B[Deng et al. 2024]	-	75.1
GeoSDF-Solving	<b>94.5</b>	<b>95.9</b>

check, and 5,697 diagrams (**81.60%**) successfully meet the target equivalence conditions.

#### 4.5 Equivalence of Synthesised GeoSDF Diagrams

To further assess whether the diagrams synthesized by GeoSDF preserve the same geometry information in the original diagrams, we conducted an experiment by replacing the geometry diagrams in the test set of GeoQA with newly synthesized versions. We then evaluated whether baseline models could still solve the problems using these new diagrams. We tested several baseline models, including NGS [Chen et al. 2021] and G-LLaVA-7B [Gao et al. 2025], using both the original and GeoSDF-synthesized test sets. All models were evaluated with their publicly released code and model weights were trained on the original training set. To create the new diagrams, we annotated problem predicates and used GeoSDF to synthesize diagrams for each test example. The results of this experiment are shown in Table 3. Interestingly, the accuracy on the GeoSDF-synthesized test set was slightly higher than on the original test set. We attribute this improvement to the fact that some of the original diagrams were of relatively low quality, which likely hindered model performance. In contrast, the diagrams synthesized by GeoSDF offer clearer visual representations, helping the models better understand the geometry and ultimately improving accuracy.

Table 3. Comparison (%) on the GeoQA test set between original diagrams and those synthesized by GeoSDF, evaluated across different base models.

Test Set	Original Test Set	Synthesised by GeoSDF
NGS [Chen et al. 2021]	60.9	61.5
SCA-GPS[Ning et al. 2023]	64.1	64.9
G-LLaVA-7B[Gao et al. 2025]	64.2	64.3

#### 4.6 Computational Efficiency and Convergence Analysis

The computational efficiency and convergence behavior of our GeoSDF framework are critical for its practical applicability. To evaluate computational performance, we compare the performance, resource usage, and rendering time versus Batch Size for the IMO level figure as shown in Tab. 4. GeoSDF could also run on the CPU or the laptop platform due to it is not sensitive to the computing power. The optimization time is nearly constant, so not included in this table because we find the bottleneck is in the transfer speed between the GPU and CPU. We measure the average optimization time for generating diverse geometric figures. For typical complex IMO level figures (e.g., those involving 20+ elements and 20+ constraints), the generation process converges in about 20s with annotations. For example, the optimization time is about 21.3s for IMO 2021 P4 for all batch size configurations with 24 elements and 24 constraints. This performance demonstrates the feasibility of our approach for interactive or near-interactive geometric design.

Table 4. Performance, Resource Usage, and Rendering Time vs. Batch Size over IMO Diagram Synthesis. The accuracy is calculated as the loss less than 0.1 in a batch. The Memory is the maximum GPU memory allocated throughout the entire process.

Batch Size	Accuracy (%)	Memory (GB)	Rendering Time (s)
2048	57.67	14.49	77.4
1024	57.42	7.02	39.2
512	56.84	3.52	21.4
256	60.16	1.77	12.3
128	60.94	0.89	7.5
64	62.19	0.50	5.2
32	53.13	0.38	4.0

#### 4.7 Impact of Crowd Regularization

We conducted an ablation study to show the contribution of the crowd regularization term (i.e., Eqn. 2) in GeoSDF. This term aims to prevent geometric elements from collapsing, encouraging well-distributed diagrams. Without the crowd term, diagrams generated on the GeoQA dataset showed a degradation, with points overlapping and lines merging. Quantitatively, this resulted in a decrease of 3.7% in the success rate of diagram synthesis on the Formal-Geo7K dataset, ranging from 77.89% to 81.60%. This unequivocally demonstrates that the crowd term is crucial for enforcing geometric separation and visual clarity for GeoSDF's robustness and efficacy in generating accurate plane geometry diagrams.

## 5 CONCLUSION

In this work, we introduced GeoSDF, a novel approach for synthesizing plane geometry diagrams by leveraging Signed Distance Field. GeoSDF can generate precise and semantically aligned diagrams, supported by an integrated self-verification mechanism that ensures consistency with the original problem constraints. By leveraging the implicit representation and differentiability of SDFs, GeoSDF enables flexible and accurate diagram synthesis. Our extensive experiments demonstrate that GeoSDF can produce high-quality diagrams, generalize well across a wide range of problems, including

complex International Mathematical Olympiad (IMO) problems, and effectively handle intricate geometric relationships and constraints. A key advantage of GeoSDF is its quantifiability, which opens up promising applications such as directly solving geometry problems. Experimental results show that GeoSDF significantly outperforms existing SOTA solvers, highlighting its strong potential to contribute to the field of solving geometry problems. Meanwhile, GeoSDF also maintains strong computational efficiency, making it well-suited for deployment across various application domains with minimal computational resource requirements. Our GeoSDF bridges the gap between computational graphics and AI4Math, offering a robust tool for advancing geometric reasoning in MLLMs and beyond. Future work will explore GeoSDF to handle more types of geometry diagrams including solid geometry and analytic geometry.

## REFERENCES

- Shuai Bai, Keqin Chen, Xuejing Liu, Jialin Wang, Wenbin Ge, Sibao Song, Kai Dang, Peng Wang, Shijie Wang, Jun Tang, Humen Zhong, Yuanzhi Zhu, Mingkun Yang, Zhaohai Li, Jianqiang Wan, Pengfei Wang, Wei Ding, Zheren Fu, Yiheng Xu, Jiabo Ye, Xi Zhang, Tianbao Xie, Zesen Cheng, Hang Zhang, Zhibo Yang, Haiyang Xu, and Junyang Lin. 2025. Qwen2.5-VL Technical Report. arXiv:2502.13923 [cs.CV] <https://arxiv.org/abs/2502.13923>
- Mark de Berg, Offried Cheong, Marc van Kreveld, and Mark Overmars. 2008. *Computational Geometry: Algorithms and Applications* (3rd ed. ed.). Springer-Verlag TELOS, Santa Clara, CA, USA.
- Shihao Cai, Keqin Bao, Hangyu Guo, Jizhi Zhang, Jun Song, and Bo Zheng. 2024. GeoGPT4V: Towards Geometric Multi-modal Large Language Models with Geometric Image Generation. In *Proceedings of the 2024 Conference on Empirical Methods in Natural Language Processing*, Yaser Al-Onaizan, Mohit Bansal, and Yun-Nung Chen (Eds.). Association for Computational Linguistics, Miami, Florida, USA, 750–766. <https://aclanthology.org/2024.emnlp-main.44>
- Jie Cao and Jing Xiao. 2022. An Augmented Benchmark Dataset for Geometric Question Answering through Dual Parallel Text Encoding. In *Proceedings of the 29th International Conference on Computational Linguistics*. 1511–1520.
- Jiaqi Chen, Jianheng Tang, Jinghui Qin, Xiaodan Liang, Lingbo Liu, Eric Xing, and Liang Lin. 2021. GeoQA: A Geometric Question Answering Benchmark Towards Multimodal Numerical Reasoning. In *Findings of the Association for Computational Linguistics: ACL-IJCNLP 2021*. Association for Computational Linguistics, Online, 513–523. <https://doi.org/10.18653/v1/2021.findings-acl.46>
- Zhe Chen, Jiannan Wu, Wenhai Wang, Weijie Su, Guo Chen, Sen Xing, Muyan Zhong, Qinglong Zhang, Xizhou Zhu, Lewei Lu, et al. 2024. Internvl: Scaling up vision foundation models and aligning for generic visual-linguistic tasks. In *Proceedings of the IEEE/CVF conference on computer vision and pattern recognition*. 24185–24198.
- Linger Deng, Yuliang Liu, Bohan Li, Dongliang Luo, Liang Wu, Chengquan Zhang, Pengyuan Lyu, Ziyang Zhang, Gang Zhang, Errui Ding, et al. 2024. R-CoT: Reverse Chain-of-Thought Problem Generation for Geometric Reasoning in Large Multimodal Models. arXiv preprint arXiv:2410.17885 (2024).
- Jiahui Gao, Renjie Pi, Jipeng Zhang, Jiacheng Ye, Wanjun Zhong, Yufei Wang, Lanqing HONG, Jianhua Han, Hang Xu, Zhenguo Li, and Lingpeng Kong. 2025. G-LLaVA: Solving Geometric Problem with Multi-Modal Large Language Model. In *The Thirteenth International Conference on Learning Representations*. <https://openreview.net/forum?id=px1674Wp3C>
- J. D. Hunter. 2007. Matplotlib: A 2D graphics environment. *Computing in Science & Engineering* 9, 3 (2007), 90–95. <https://doi.org/10.1109/MCSE.2007.55>
- Mehran Kazemi, Hamidreza Alvari, Ankit Anand, Jialin Wu, Xi Chen, and Radu Soric. 2024. GeomVerse: A Systematic Evaluation of Large Models for Geometric Reasoning. In *AI for Math Workshop@ ICML 2024*.
- Haotian Liu, Chunyuan Li, Yuheng Li, and Yong Jae Lee. 2023. Improved Baselines with Visual Instruction Tuning. arXiv:2310.03744 [cs.CV]
- Pan Lu, Hritik Bansal, Tony Xia, Jiacheng Liu, Chunyuan Li, Hannaneh Hajishirzi, Hao Cheng, Kai-Wei Chang, Michel Galley, and Jianfeng Gao. 2024. MathVista: Evaluating Mathematical Reasoning of Foundation Models in Visual Contexts. In *International Conference on Learning Representations (ICLR)*.
- Pan Lu, Ran Gong, Shibiao Jiang, Liang Qiu, Siyuan Huang, Xiaodan Liang, and Song-Chun Zhu. 2021. Inter-GPS: Interpretable Geometry Problem Solving with Formal Language and Symbolic Reasoning. In *The Joint Conference of the 59th Annual Meeting of the Association for Computational Linguistics and the 11th International Joint Conference on Natural Language Processing (ACL-IJCNLP 2021)*.
- Maizhen Ning, Qiu-Feng Wang, Kaizhu Huang, and Xiaowei Huang. 2023. A symbolic characters aware model for solving geometry problems. In *Proceedings of the 31st ACM International Conference on Multimedia*. 7767–7775.
- Maizhen Ning, Zihao Zhou, QiuFeng Wang, Xiaowei Huang, and Kaizhu Huang. 2025. GNS: Solving Plane Geometry Problems by Neural-Symbolic Reasoning with Multi-Modal LLMs. In *Proceedings of the AAAI Conference on Artificial Intelligence*, Vol. 39. 24957–24965.
- OpenAI. 2024. DALL-E 3. In <https://openai.com/index/dall-e-3/>.
- Robin Rombach, Andreas Blattmann, Dominik Lorenz, Patrick Esser, and Björn Ommer. 2021. High-Resolution Image Synthesis with Latent Diffusion Models. arXiv:2112.10752 [cs.CV]
- Robin Rombach, Andreas Blattmann, Dominik Lorenz, Patrick Esser, and Björn Ommer. 2022. High-resolution image synthesis with latent diffusion models. In *Proceedings of the IEEE/CVF conference on computer vision and pattern recognition*. 10684–10695.
- Minjoon Seo, Hannaneh Hajishirzi, Ali Farhadi, Oren Etzioni, and Clint Malcolm. 2015. Solving geometry problems: Combining text and diagram interpretation. In *Proceedings of the 2015 conference on empirical methods in natural language processing*. 1466–1476.
- Min Joon Seo, Hannaneh Hajishirzi, Ali Farhadi, and Oren Etzioni. 2014. Diagram understanding in geometry questions. In *Proceedings of the AAAI Conference on Artificial Intelligence*, Vol. 28.
- Haizhou Shi, Zihao Xu, Hengyi Wang, Weiyei Qin, Wenyuan Wang, Yibin Wang, Zifeng Wang, Sayna Ebrahimi, and Hao Wang. 2024. Continual learning of large language models: A comprehensive survey. arXiv preprint arXiv:2404.16789 (2024).
- GeoGebra Team. 2024. GeoGebra - Dynamic Mathematics for Everyone. <https://www.geogebra.org/>.
- Trieu Trinh, Yuhuai Wu, Quoc Le, He He, and Thang Luong. 2024. Solving Olympiad Geometry without Human Demonstrations. *Nature* (2024). <https://doi.org/10.1038/s41586-023-06747-5>
- Renqiu Xia, Mingsheng Li, Hancheng Ye, Wenjie Wu, Hongbin Zhou, Jiakang Yuan, Tianshuo Peng, Xinyu Cai, Xiangchao Yan, Bin Wang, Conghui He, Botian Shi, Tao Chen, Junchi Yan, and Bo Zhang. 2025. GeoX: Geometric Problem Solving Through Unified Formalized Vision-Language Pre-training. In *The Thirteenth International Conference on Learning Representations*. <https://openreview.net/forum?id=6RiB15sCDF>
- Shihao Xu, Yiyang Luo, and Wei Shi. 2024a. Geo-LLaVA: A Large Multi-Modal Model for Solving Geometry Math Problems with Meta In-Context Learning. In *Proceedings of the 2nd Workshop on Large Generative Models Meet Multimodal Applications*. 11–15.
- Shihao Xu, Yiyang Luo, and Wei Shi. 2024b. Geo-LLaVA: A Large Multi-Modal Model for Solving Geometry Math Problems with Meta In-Context Learning. In *Proceedings of the 2nd Workshop on Large Generative Models Meet Multimodal Applications*. 11–15.
- Lior Yariv, Yoni Kasten, Daniel Moran, Meirav Galun, Lior Wolf, and Ron Kimmel. 2020. Multiview neural surface reconstruction by disentangling geometry and appearance. *Advances in Neural Information Processing Systems* 33 (2020), 2492–2502.
- Jiaxin Zhang, Zhong-Zhi Li, Ming-Liang Zhang, Fei Yin, Cheng-Lin Liu, and Yashar Moshfeghi. 2024b. GeoEval: Benchmark for Evaluating LLMs and Multi-Modal Models on Geometry Problem-Solving. In *Findings of the Association for Computational Linguistics ACL 2024*. 1258–1276.
- Lvmin Zhang, Anyi Rao, and Maneesh Agrawala. 2023a. Adding conditional control to text-to-image diffusion models. In *Proceedings of the IEEE/CVF international conference on computer vision*. 3836–3847.
- Renrui Zhang, Dongzhi Jiang, Yichi Zhang, Haokun Lin, Ziyu Guo, Pengshuo Qiu, Aojun Zhou, Pan Lu, Kai-Wei Chang, Yu Qiao, et al. 2024a. Mathverse: Does your multi-modal llm truly see the diagrams in visual math problems?. In *European Conference on Computer Vision*. Springer, 169–186.
- Renrui Zhang, Xinyu Wei, Dongzhi Jiang, Ziyu Guo, Shicheng Li, Yichi Zhang, Chengzhuo Tong, Jiaming Liu, Aojun Zhou, Bin Wei, et al. 2024c. MAVIS: Mathematical Visual Instruction Tuning with an Automatic Data Engine. arXiv preprint arXiv:2407.08739 (2024).
- Xiaokai Zhang, Na Zhu, Yiming He, Jia Zou, Qike Huang, Xiaoxiao Jin, Yanjun Guo, Chenyang Mao, Zhe Zhu, Dengfeng Yue, et al. 2023b. FormalGeo: The First Step Toward Human-like IMO-level Geometric Automated Reasoning. arXiv e-prints (2023), arXiv–2310.
- Wenwen Zhuang, Xin Huang, Xiantao Zhang, and Jin Zeng. 2024. Math-PUMA: Progressive Upward Multimodal Alignment to Enhance Mathematical Reasoning. arXiv preprint arXiv:2408.08640 (2024).



Fig. 7. A batch of synthesis diagrams. Source from IMO 2021 Problem 4.



Fig. 8. A batch of synthesis diagrams. Synthesis from IMO 2022 Problem 4.